Single photon timing resolution and detection efficiency of the ITC-IRST silicon photo-multipliers

Gianmaria Collazuol
Scuola Normale Superiore and INFN Pisa

on behalf of
G.Ambrosi, M.Boscardin, F.Corsi, G.F.Dalla Betta, A.Del Guerra, M.Galimberti, D.Giulietti, L.A.Gizzi, L.Labate, G.Llosa, S.Marcatili, C.Piemonte, A.Pozza, N.Zorzi

Overview

- The SiPM devices produced at IRST
- Photodetection efficiency
- Single photon timing resolution
- Energy resolution of SiPM coupled to LSO
- Next steps, improvements and Conclusions

The IRST SiPM technology

The SiPM building block
Shallow-Junction GM-APD

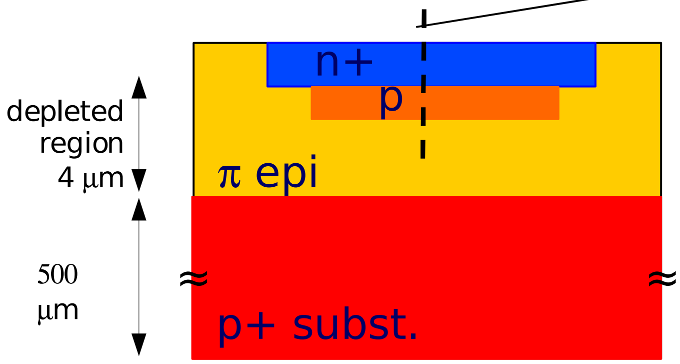

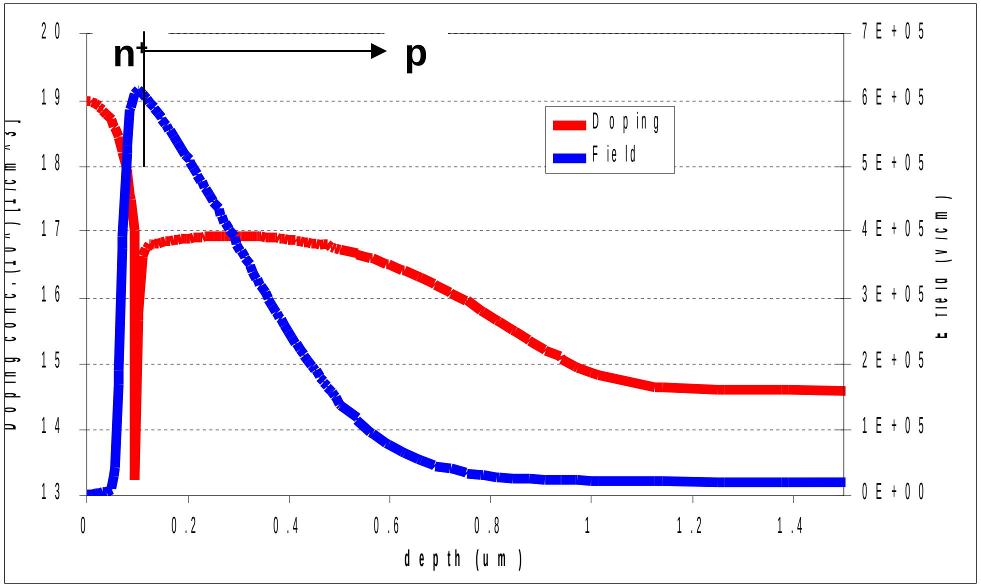

Optimization for the blue light (420nm)

1) Substrate: p-type epitaxial
2) Very thin (100nm) n^+ layer
3) Quenching resistance made of doped polysilicon
4) Anti-reflective coating (ARC) optimized for $\lambda \sim 420$nm
5) Geometry (fill factor) NOT yet optimized for maximum PDE
6) Trenches for optical insulation of cell (low cross-talk)

C.Piemonte et al. IEEE TNS (2007)

The IRST technology

Since the beginning of project (2005) three batches with the same layuot have been produced:

- to verify functionalities and reproducibility of the production processes
- to study the technology for dark count rate and reducing optical cross-talk
- to investigate the photodetection efficiency

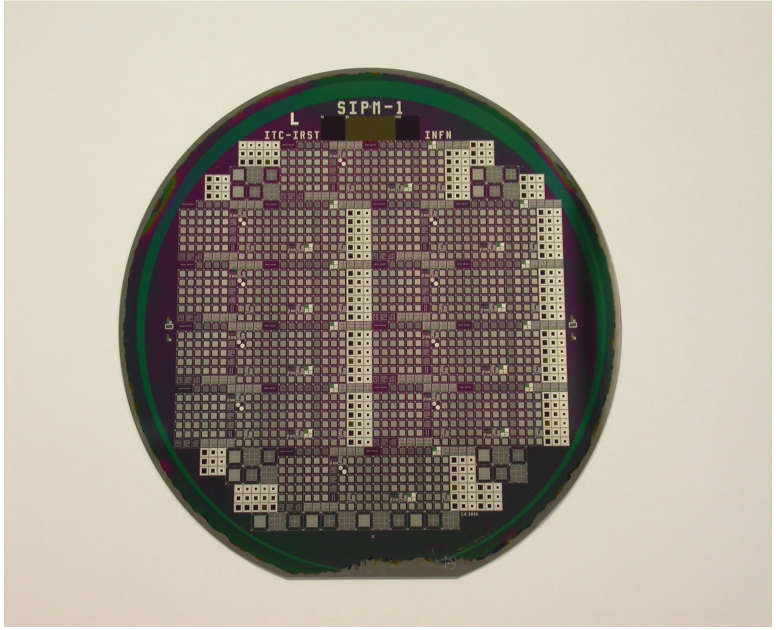

The wafer layout includes many structures:

- SiPMs
- single GM-APDs
- "large-area" diodes (no R_{quench})
- + several test structures

Basic SiPM geometry:

- 25x25 cells
- cell size: 40x40 μm^2

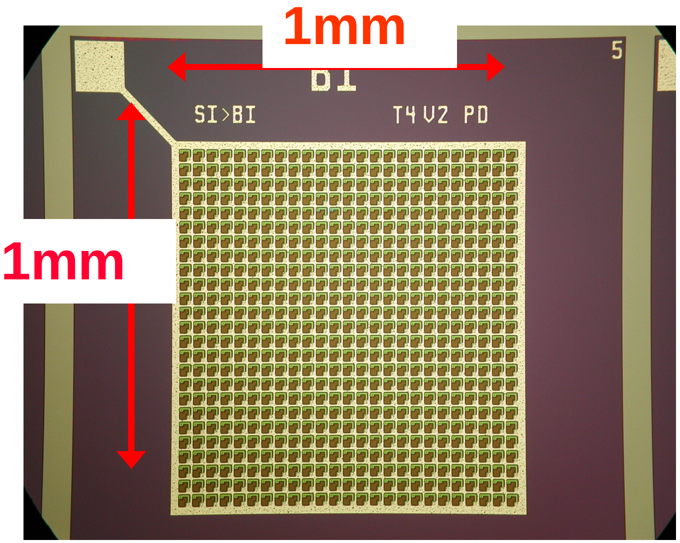

Characterization of the devices

Gain

related to the recharge of the diode capacitance from V_{BD} to V_{bias} during the avalanche quenching time after I_{latch} is reached.

$G=(V_{BIAS}-V_{BD}) * C_D/q$

valid for few volts above V_{BD}

Noise: dark count

pulses triggered by non-photogenerated carriers (thermal generation in the bulk or in the surface depeted region around the junction)

afterpulse

carriers can be trapped during an avalanche and then released triggering another avalanche

optical cross-talk

photoegeneration during the avalanche discharge. Some of the photons can be absorbed in the adjacent cell possibly triggering new discharges

Photodetection efficiency

$PDE = QE * P_{trigg} * \varepsilon_{geom}$

QE = quantum efficiency

P_{trigg} = avalanche triggering prob.

ε_{geom} = geometrical fill factor

Time resolution

Related to the photogeneration and to the avalange propagation

Static characteristics (I-V measurement)

Fast tests to verify the functionality of the device:

- Breakdown voltage (V_{bd})
- Dark count rate (N_{dark})
- Quenching resistor value R_Q

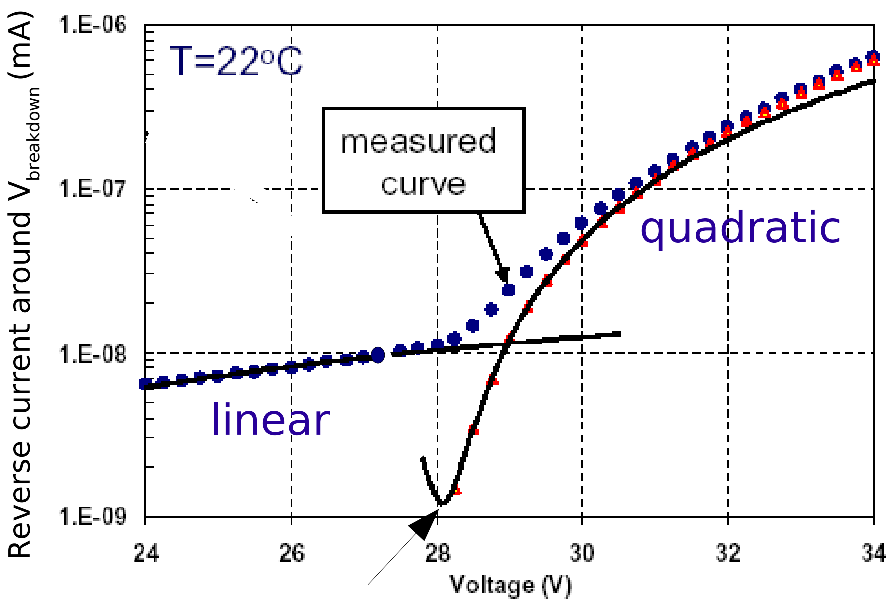

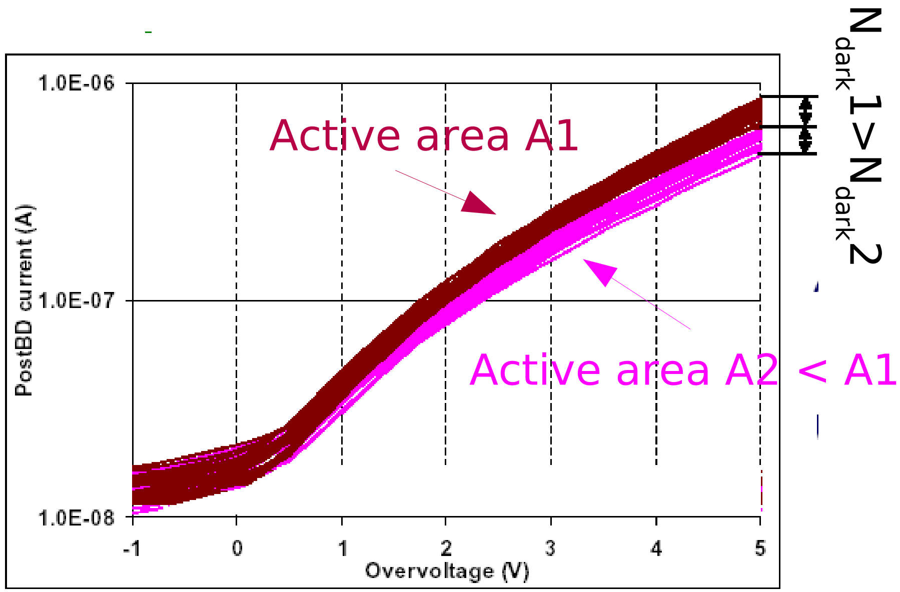

Pre-breakdown: current mainly due to generation in the surface region around diode:

$I_{pre\text{-}BD} \sim V_{bias}$ (linear)

Post-breakdown: up to few V current due dark events is:

$I_{post\text{-}BD} = q \cdot G \cdot N_{dark} \sim q \cdot V_{bias} \cdot V_{bias}$ (quadratic)

- Uniform breakdown voltage in a wafer and from wafer to wafer.
- post-breakdown current very uniform → uniform dark count rate
- less than 20% of the devices show anomalous current behavior (~1000 devices measured)

C.Piemonte et al. IEEE NSS 2006 CD record N42-4 and IEEE TNS (2007)

Dynamic characteristics

Complete characterization of signal and noise:
Signal shape, gain, dark noise rate, optical cross-talk, after-pulse

The signal presents 2 components:

1. fast component: avalanche current reproduced at the output by parasitic capacitor

2. slow component due to the recharge of the diode capacitance (recovery time ~70ns)

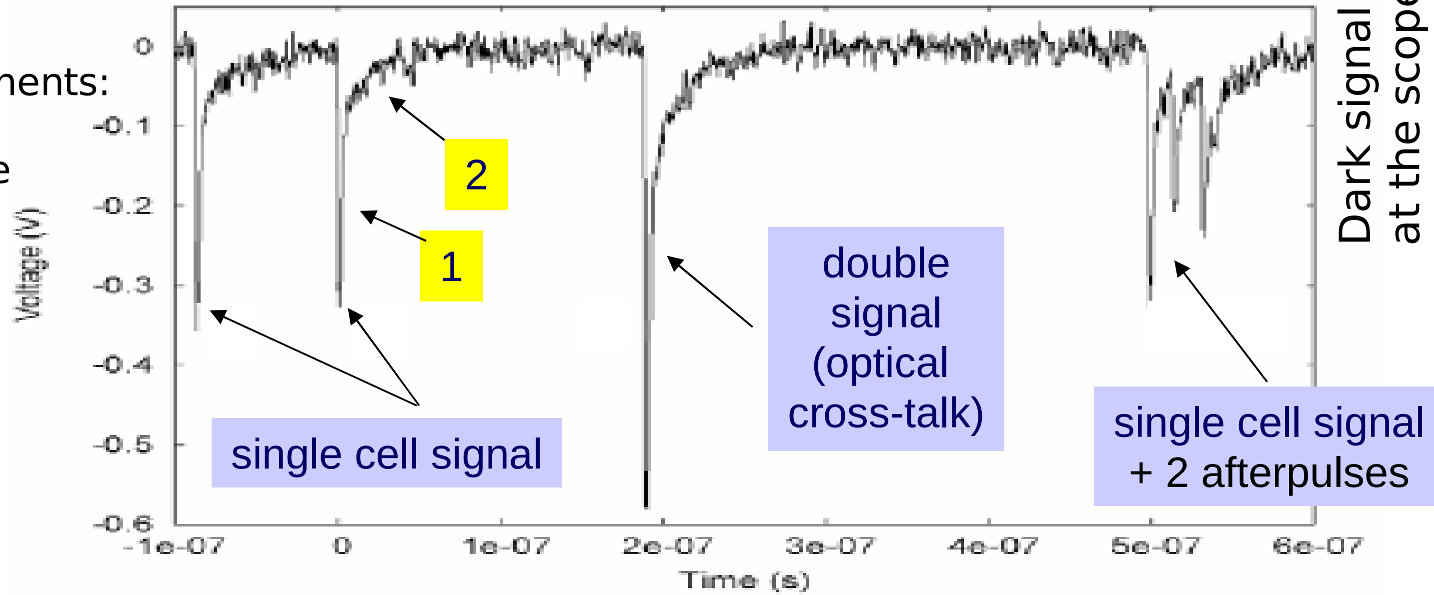

Dark signal at the scope

Gain is linear up to ~ 5V overvoltage
→ effective avalanche quenching

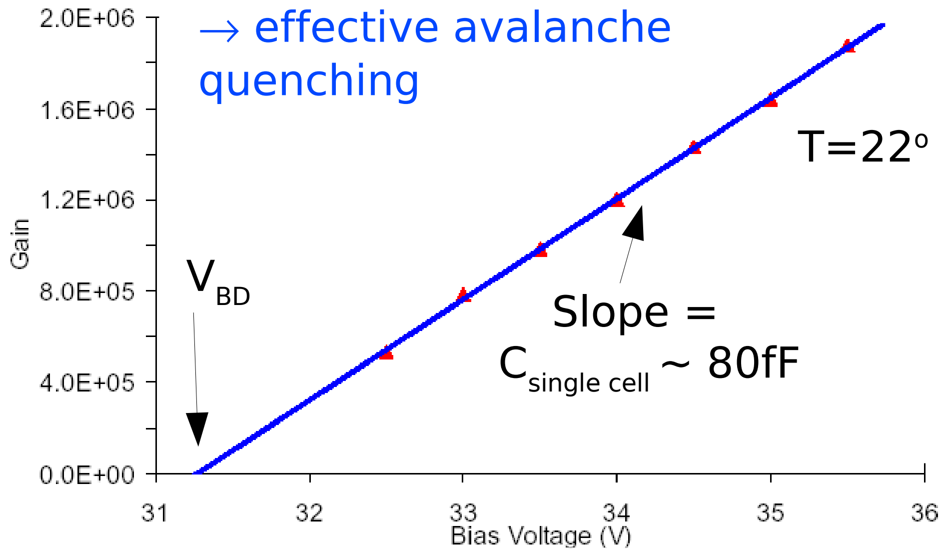

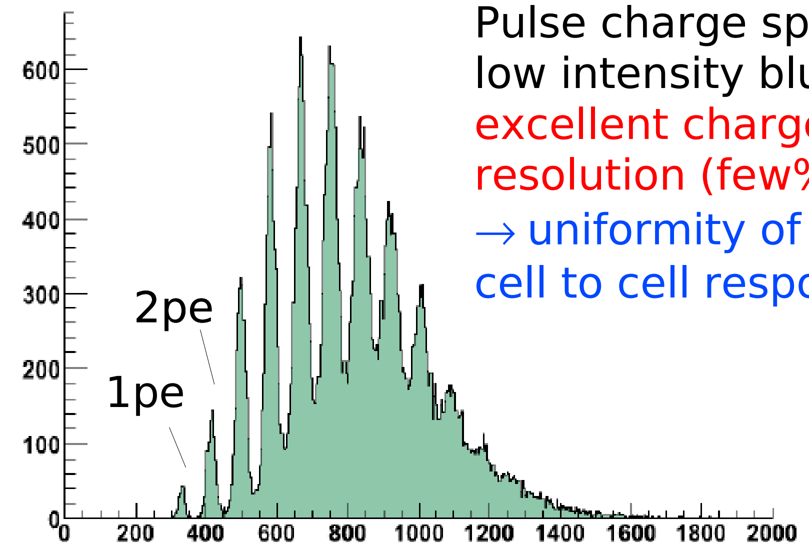

Pulse charge spectrum low intensity blue LED
excellent charge resolution (few%)
→ uniformity of cell to cell response

Photodetection efficiency (PDE)

$$PDE = N_{pulses} / N_{photons} =$$

Carrier Photogeneration

(QE = probability for a photon to generate a carrier that reaches the high field region)

*

Avalanche triggering

(P_{trigg} = probability for a carrier traversing the high-field to generate the avalanche)

*

Geometrical factor

(ε_{geom} = fraction of dead area due to structures between the cells, eg. guard rings, trenches)

W.Oldham et al. IEEE Trans. ED (1972)

C.Piemonte, NIM A568 (2006) 224-232

Optimization

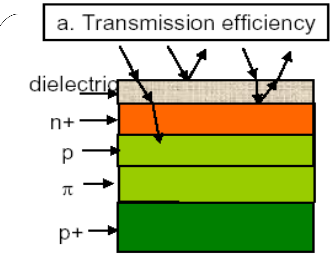

- Anti-reflective coating (ARC)

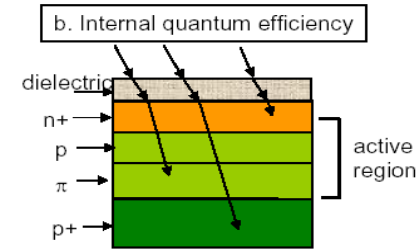

- Shallow junctions for short λ
- thick epi layers for long λ

- high overvoltage
- photogeneration in the junction p-side

Ionization rate in Si

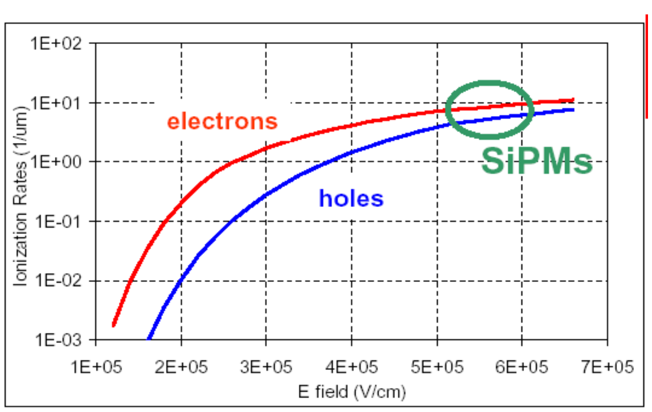

Experimental Method

Two methods: DC current and Pulses count

$$(1) \quad N_{\text{det. photons } [s^{-1}]} = \frac{I_{\text{light}} - I_{\text{dark}}}{q \cdot G}$$

$$(2) \quad N_{\text{det. photons } [s^{-1}]} = \text{Rate}_{\text{light}} - \text{Rate}_{\text{dark}}$$

$$PDE = \frac{N_{\text{detected photons}}}{N_{\text{incident photons}}}$$

Reference by calibrated detector (photodiode)

$$N_{\text{incident photons } [s^{-1} mm^{-2}]} = \Phi_{[W/mm^2]} \frac{\lambda}{hc}$$

$$\Phi_{[W/mm^2]} = \alpha_{[W/A]} \frac{I_{[A]}}{S_{[mm^2]}}$$

NOTE:

- Rate effects, afterpulses, and cross-talk must be properly taken into account. Easier for method (2).
- Method (1) needs also Gain to be measured.
- Method (2): rates of counts above 0pe can me measured. As an alternative the rate of 0pe in proper gate can be used to measure N_{pe} following Poisson statistics

Experimental Setup (IRST)

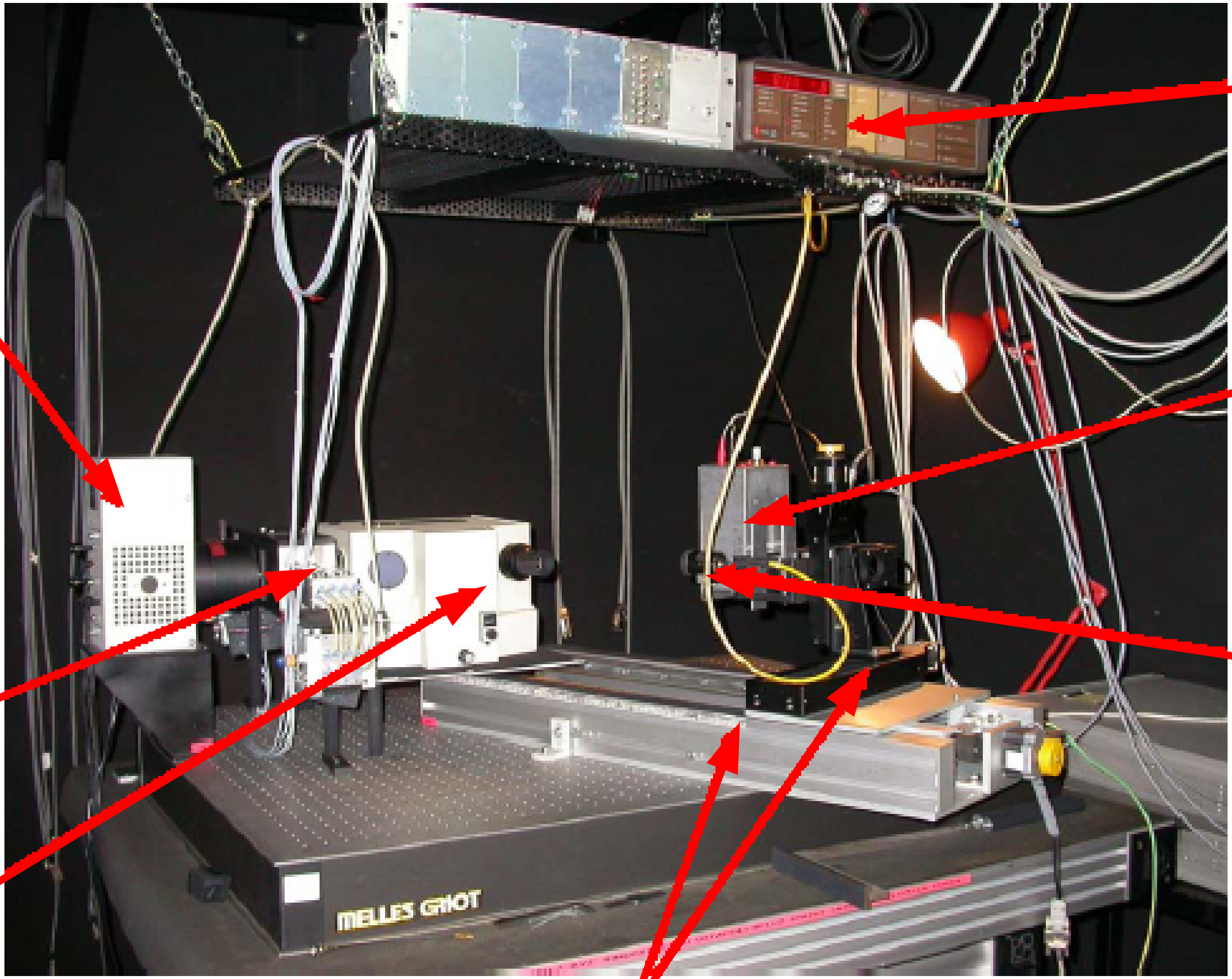

Optometer

Halogen white lamp

SiPM+ preamplifier

Neutral filters (transmittance 10%)

Photodiode UDT221

Monocromator

Stage with 3D micrometers movement (50um precision)

PDE measurement: DC vs Pulse methods

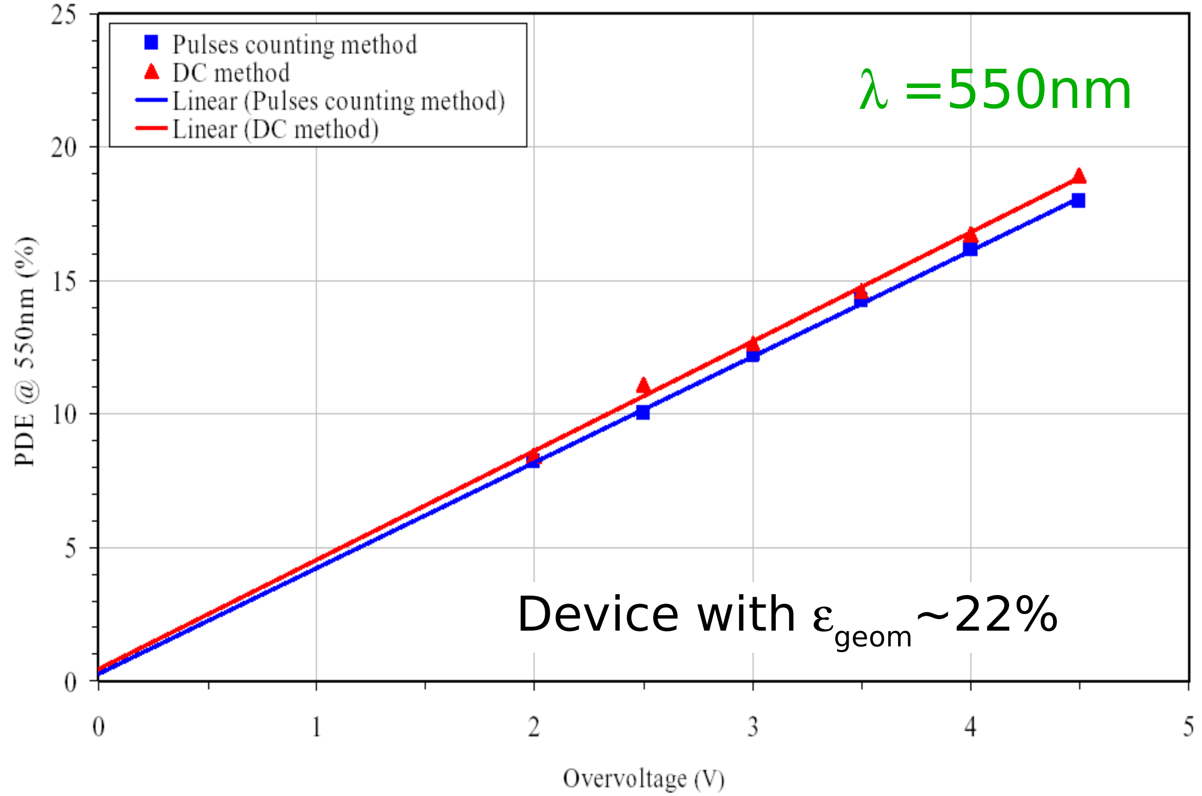

- Agreement between the two methods
- PDE ~ linear with overvoltage

C.Piemonte et al. IEEE NSS 2006 CD record 42-4

PDE vs wavelength

Flat factor

device with $\varepsilon_{geom} \sim 22\%$ not yet optimized !!!

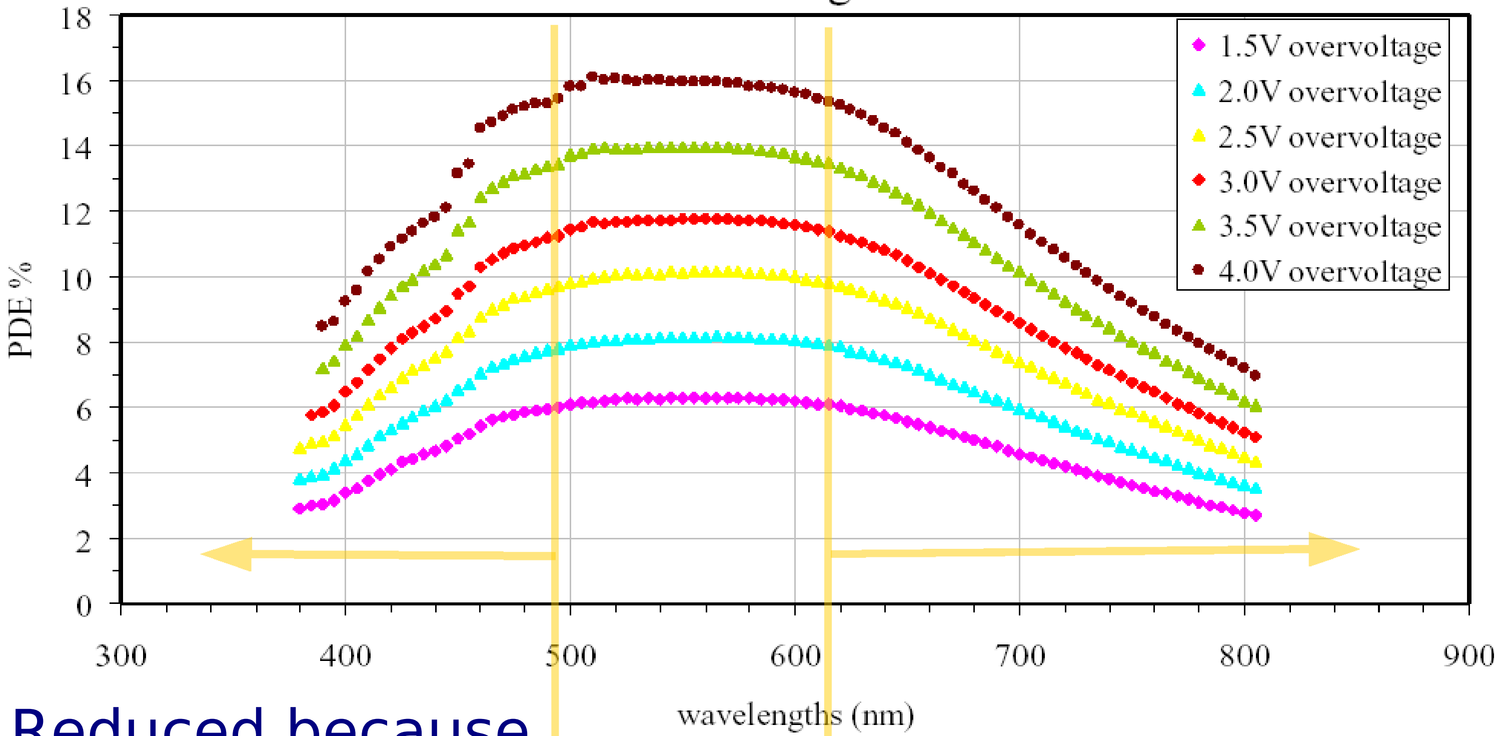

Reduced because avalanche triggered by holes

Reduced because low QE

C.Piemonte et al. IEEE NSS 2006 CD record N42-4

PDE of a single diode (photovoltaic regime)

Disentangling the 3 PDE components: no P_{trigg} and fill factor ε_{geom} here !

Direct access to internal QE and transmission trough ARC by measuring (V_{bias}~ few V) photon detection efficiency of a diode with the same n^+/p junction structure and same ARC

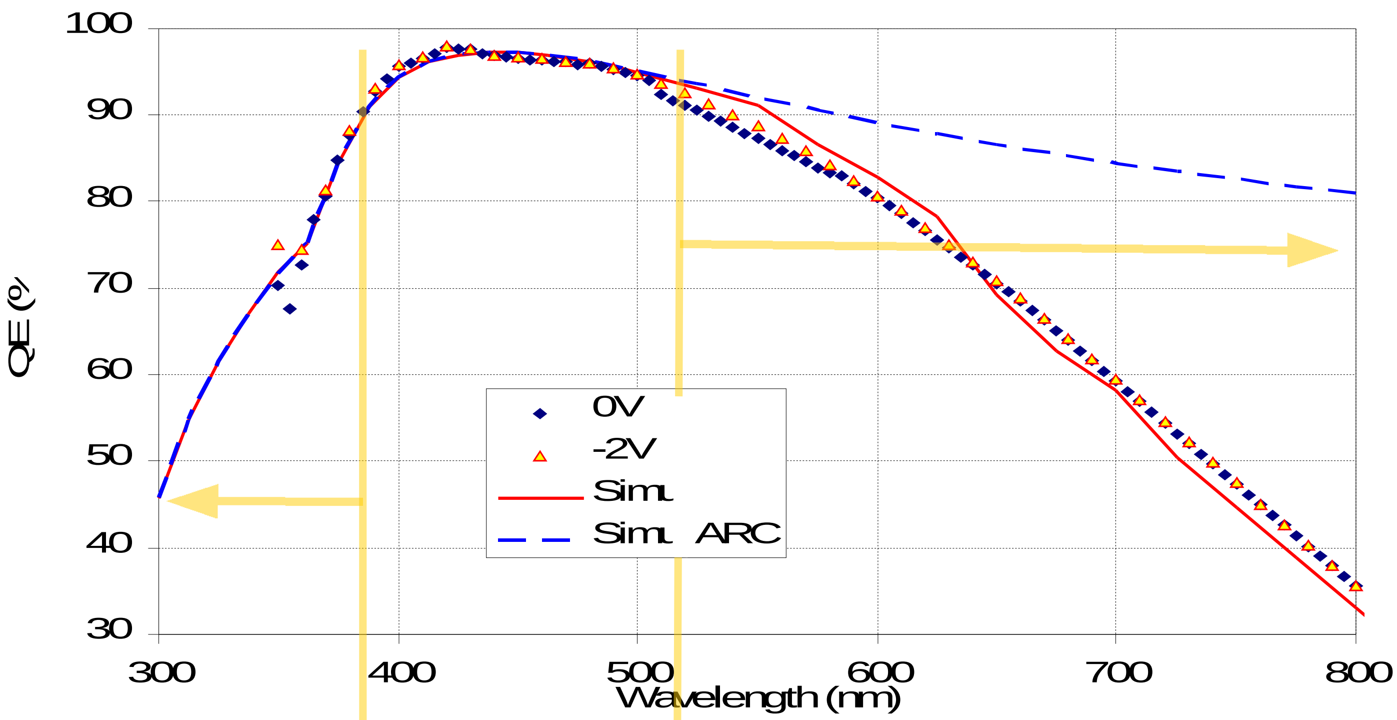

Reduced by ARC Trasmission

Reduced by small epi layer thickness

Avalanche trigger probability

$$P_{trigg} = PDE / QE / \varepsilon_{geom.}$$

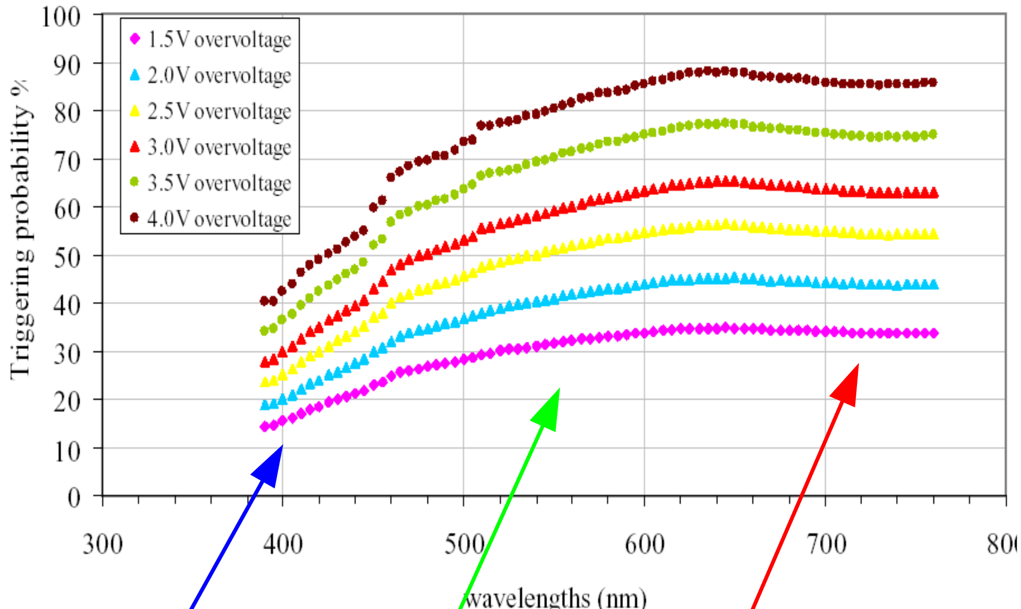

PDE ~ P_{trigg} ~ linear with overvoltage

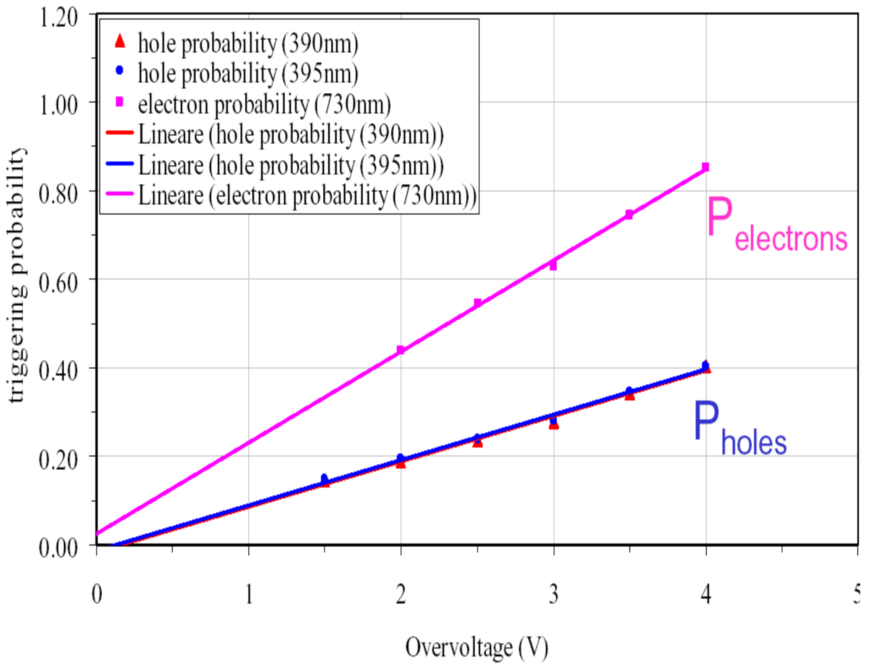

Only e⁻ cross the high E field region and trigger the avalanche

Both h⁺ and e⁻ might trigger the avalanche (but cross only a fraction of high field region)

Only h⁺ cross the high E field trigger the avalanche

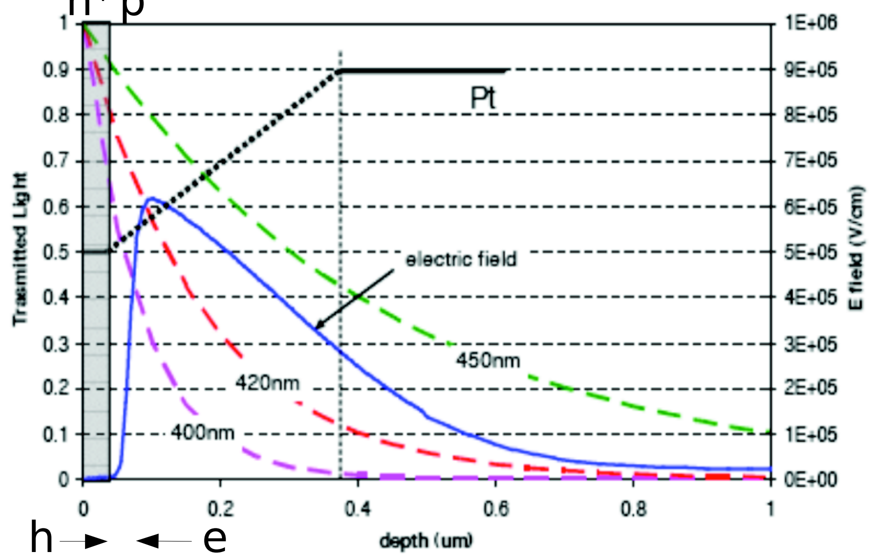

Single photon timing resolution

Detailed studies about timing of Single Photon Avalange Diodes (SPAD) by Cova et coll.

Fast component (time scale few 10ps)
main resolution peak width

Statistical fluctuations in the Avalanche:

- Vertical build-up (minor contribution)
- Horizontal propagation (major contribution)
  - via Multiplication assisted diffusion (dominating contribution)

    A.Lacaita et al. APL and El.Lett. 1990
  - via Photon assisted propagation

    PP.Webb, R.J. McIntyre RCA Eng. 1982
    A.Lacaita et al. APL 1992

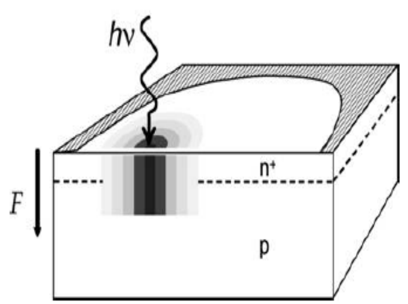

Multiplication assisted diffusion

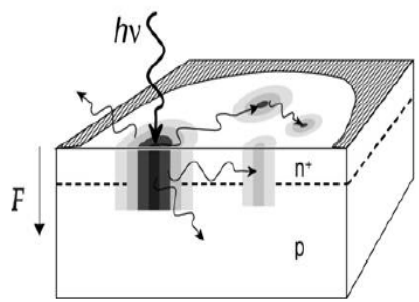

Photon assisted propagation

High overvoltage → improved time resolution

Slow component (time scale ns)
minor non gaussian tails

Carriers photogenerated in the neutral regions beneath the junction and reaching the electric field region by diffusion

G.Ripamonti, S.Cova Sol.State Electronics (1985)

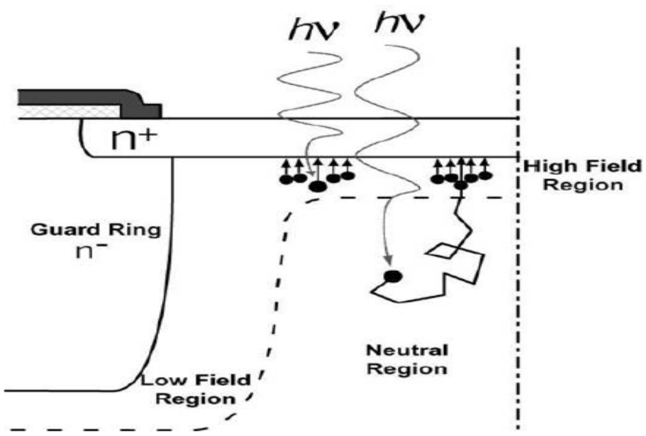

tail lifetime: $\tau \sim L^2 / \pi^2 D$

L = effective neutral layer thickness
D = diffusion coefficient

S.Cova et al. NIST Workshop on SPD (2003)

Higher resolution for short wavelengths

Experimental Method

- SiPM exposed to pulsed femto-second laser in low light intensity conditions (single photon)
- SiPM signal is sampled at high rate and the time of the pulses measured by waveform analysis
- Time resolution measured by studying the distribution of time differences between successive pulses (on the same SiPM device)

Experimental Setup (CNR Pisa)

Pump Laser
Millenia V (Spectra-physics)
solid state CW visible laser

Crystal for Second Harmonic Generation (SHG)
conversion 800 nm → 400 nm
efficiency at % level

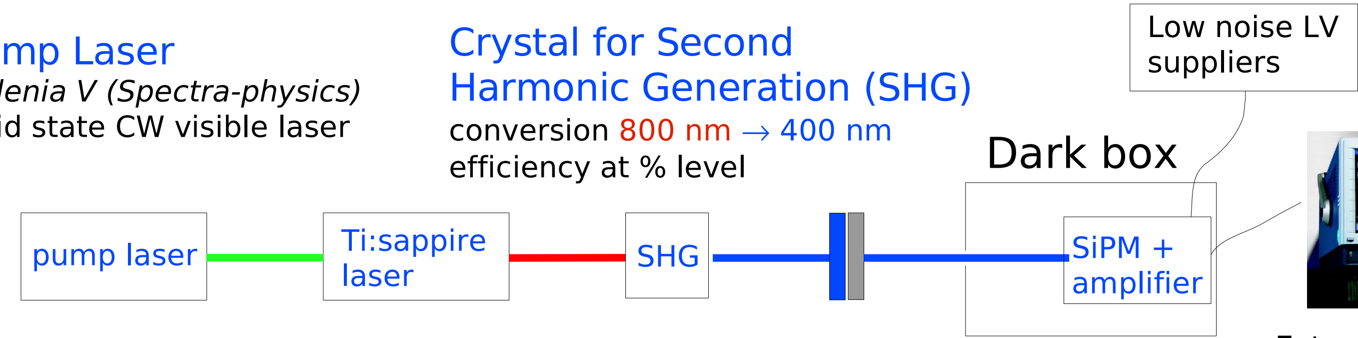

LeCroy SDA 6020

Analog bandwidth: 6GHz
Sampling rate: 20GS/s
Vertical resolution: 8 bits

(Aknowledments: E.Marcon, LeCroy)

External trigger from Ti:sappire laser signal

Mode-locked Ti:sapphire Laser
Tsunami (Spectra-physics)
femtosecond pulsed laser

Filters
blue + neutral
for rejecting IR light and tune intensity

wavelength: tuned at 800±15 nm
pulse width: ~ 60 fs
pulse period: ~ 80MHz
pulse timing jitter < 100 fs

Electronics
I → V conversion via R_L (500Ω)
Two stage voltage amplification (= x50) based on high-bandwidth low-noise RF amplifier: gali-5 (MiniCircuit)
Z_{in} = 50Ω

(Aknowledments: F.Morsani and L.Zaccarelli, INFN-Pisa)

Data taking conditions:

- different V_{bias}
- both at 800 nm and 400 nm
- with different light intensities (counting rates in the range 10÷20 Mhz ie 15÷30 KHz per single cell)

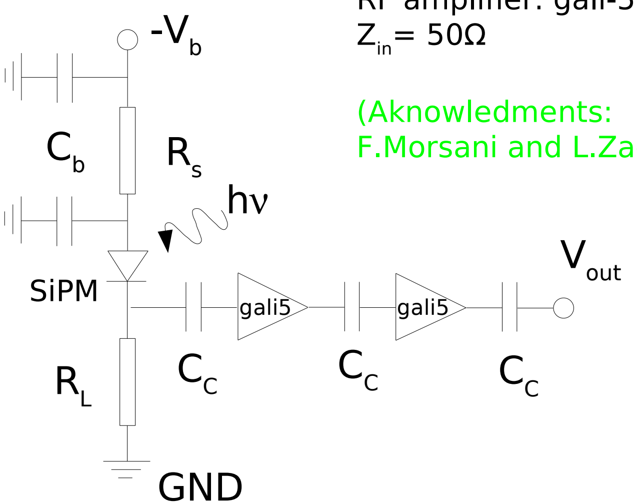

Waveform analysis

(1) Selection of candidate peaks:
- single photon peaks
- proper signal shape
- low instantaneous intensity
  (no activity before/after within 50ns)
- low noise during the previous 10 ns
  (typical noise ~ 1mV rms)

(2) Peak reconstruction
- optimum time reconstruction
- amplitude and width (baseline shift correction)

(3) Time difference Δt between consecutive peaks

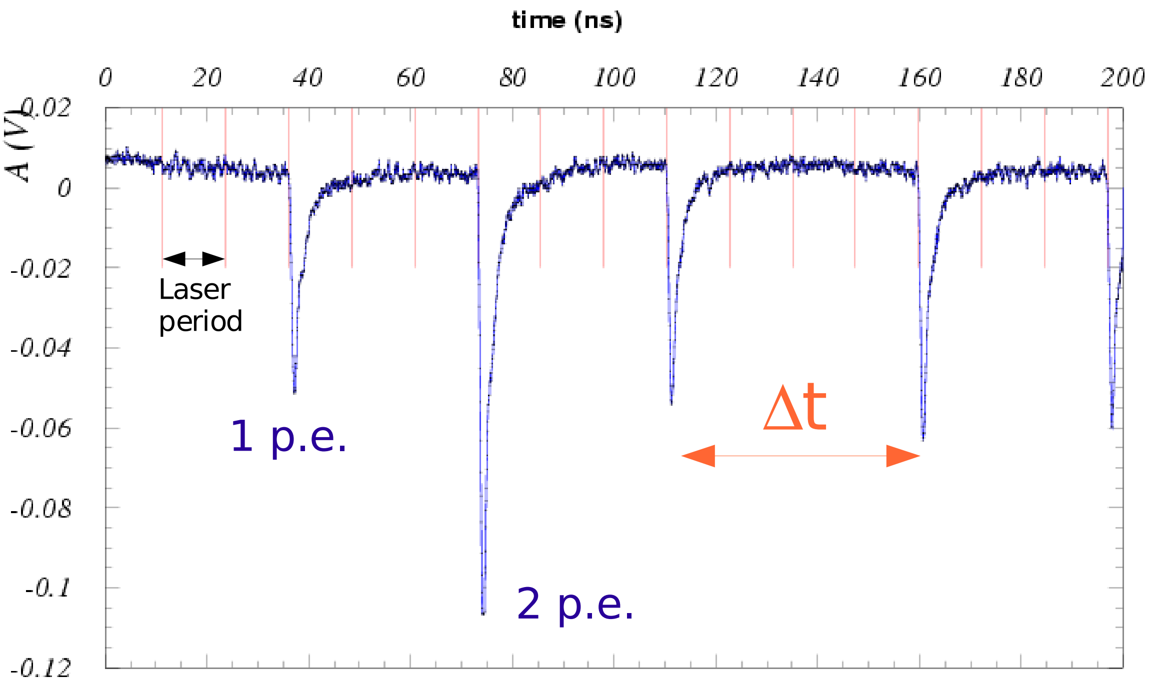

Waveform analysis: time reconstruction

Different methods to reconstruct the time of a peak:

✗ parabolic fit to find the peak maximum
✗ average of time samples weighted by the waveform derivative
✔ digital filter: weighting by the derivate of a reference signal
→ best against noise (signal shape known)

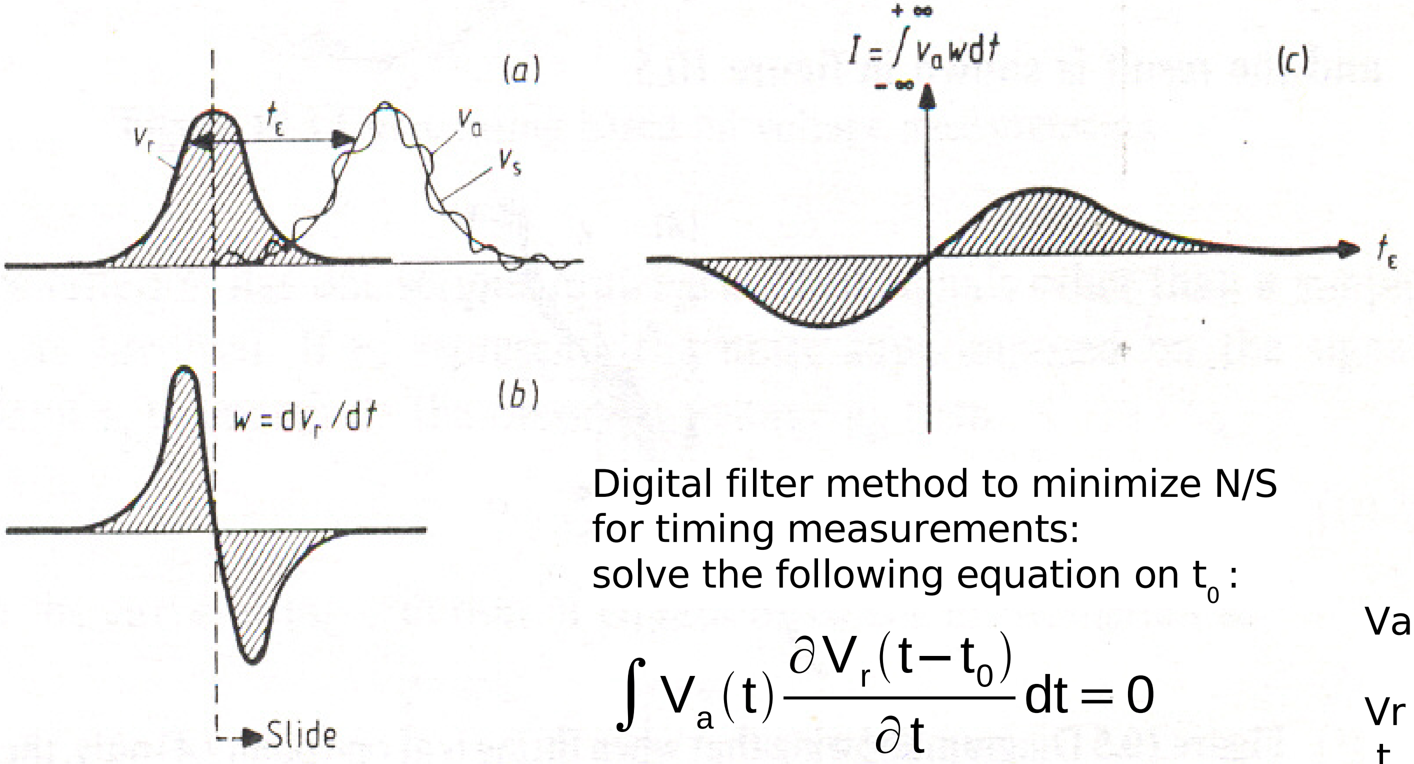

Digital filter method to minimize N/S for timing measurements:
solve the following equation on t_0 :

$$\int V_a(t)\frac{\partial V_r(t-t_0)}{\partial t}dt = 0$$

Va = measured signal (includes noise)
Vr = reference signal
t_0 = reference time

Distribution of the time differences

Distributions of the difference in time between successive peaks (modulo the measured laser period T_{laser}=12.367ns)

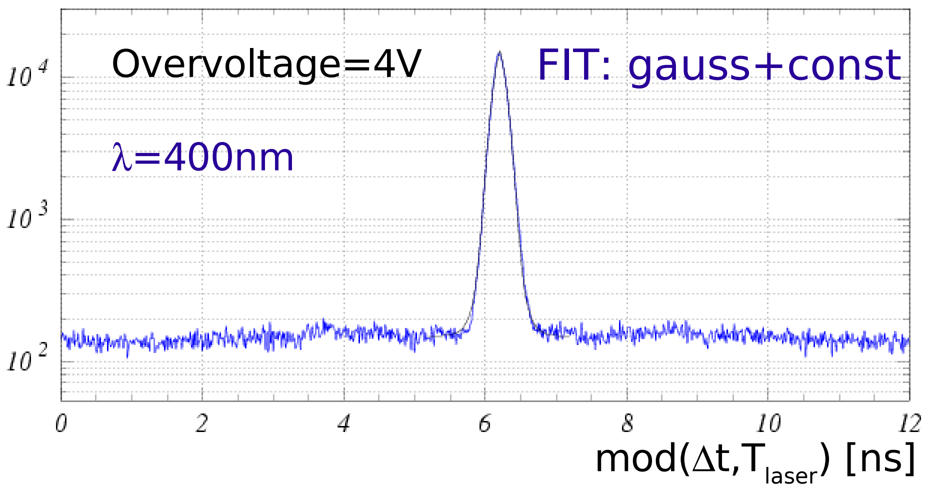

Data at λ=400nm fit gives reasonable χ^2 with gaussian (σ_t^{fit}) + constant term (dark noise contribution)

The detector resolution is obtained by $\sigma_t^{fit}/\sqrt{2}$

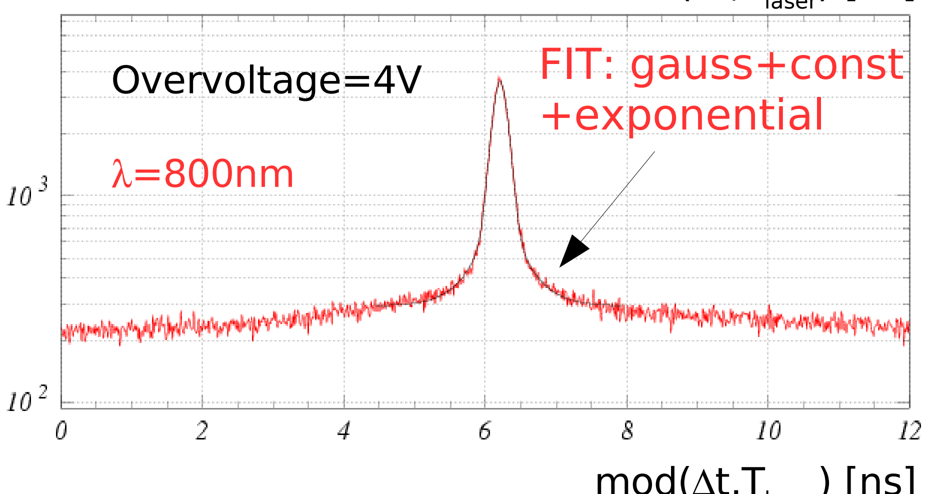

Data at λ=800nm fit gives reasonable χ^2 with an additional exponential term $\exp(-\Delta t/\tau)$

- $\tau \sim 0.2 \div 0.8$ns in rough agreement with diffusion tail lifetime: $\tau \sim L^2 / \pi^2 D$ if L is taken to be the diffusion length
- Contribution from the tails ~ 10÷30% of the resolution function area

(to be studied in detail: WORK in PROGRESS)

Time differences distribution

Cross check: SiPM coupled to a fast plastic scintillator 2 x 2 x 15mm^3
Only the scintillator exposed to the laser blue light λ=400nm.
No direct laser light to the SiPM

$\rightarrow$ measurement of the scintillator decay tail

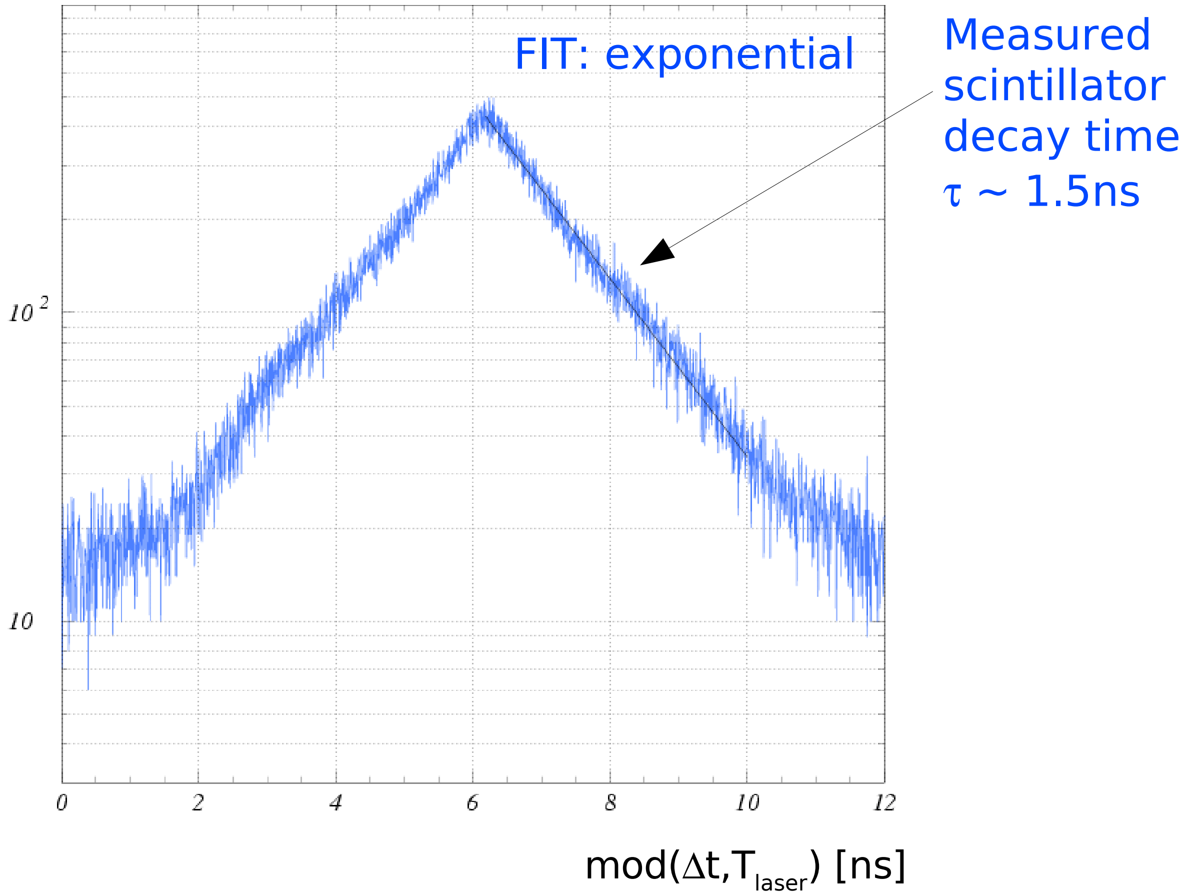

Results on IRST devices: gaussian σ_t

SiPM type without optical trench

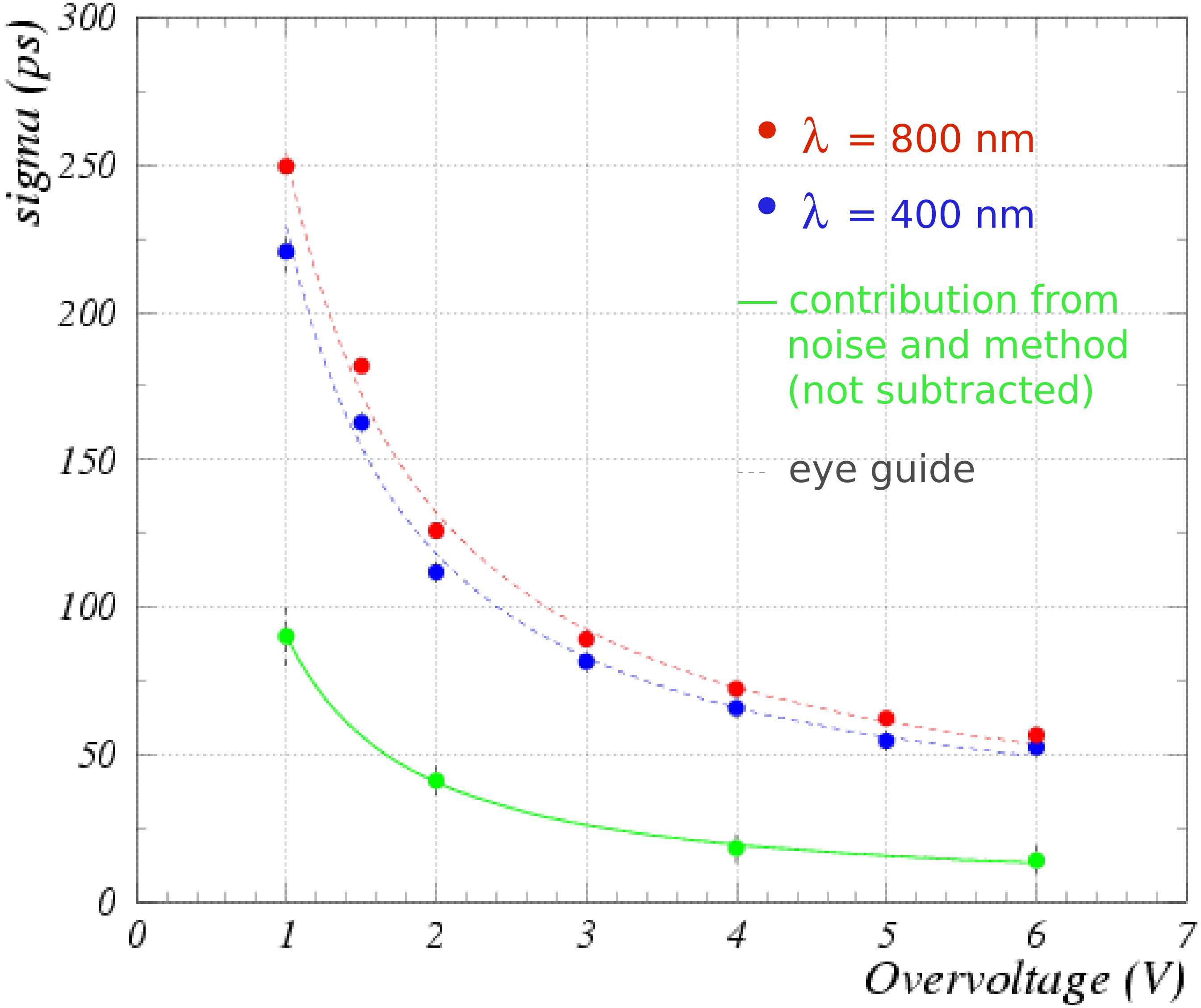

Systematics

- Contribution (main) form the electronic noise:

  (1) directly measured by splitting in two the signal of the SiPM, delaying one and recombine the two signals again. Measure the (fixed) time difference.

  (2) cross-check by doubling the noise and measuring the effect on the resolution

  This contibution includes also the systematics related to the method of time reconstruction by waveform analysys

- Contribution from sampling hardware (clock jitter, ...) < 5ps

- Sensitivity to the shape of the reference waveform < 5ps

- Systematics from fit procedure < 5ps

- Systematics from intensity dependence ~ 5ps

Other IRST devices

SiPM type without optical trench | SiPM type with optical trench

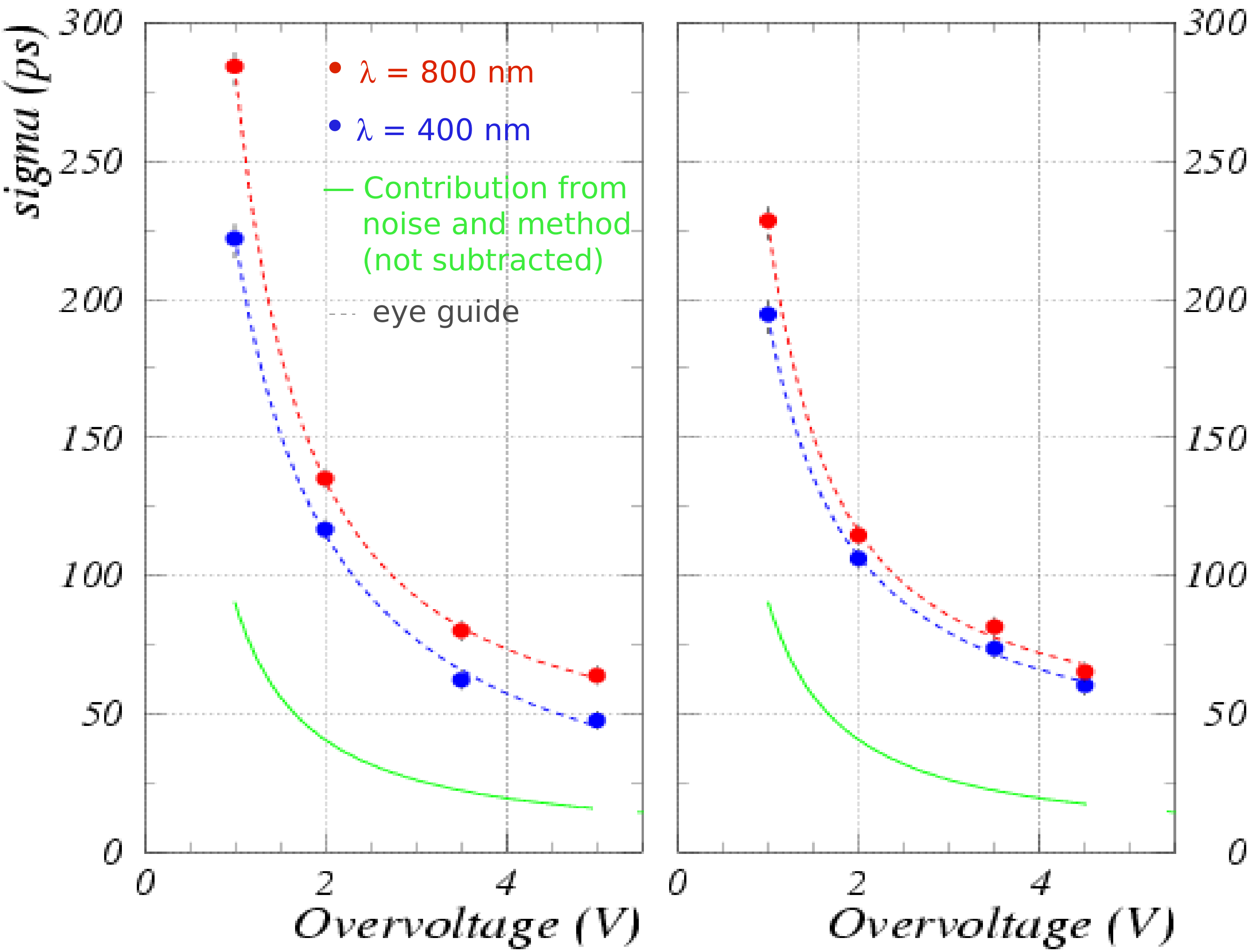

Results in fair agreement for devices with the same structure

Better resolution for short wavelengths: carriers generated next to the peak of high E field ...

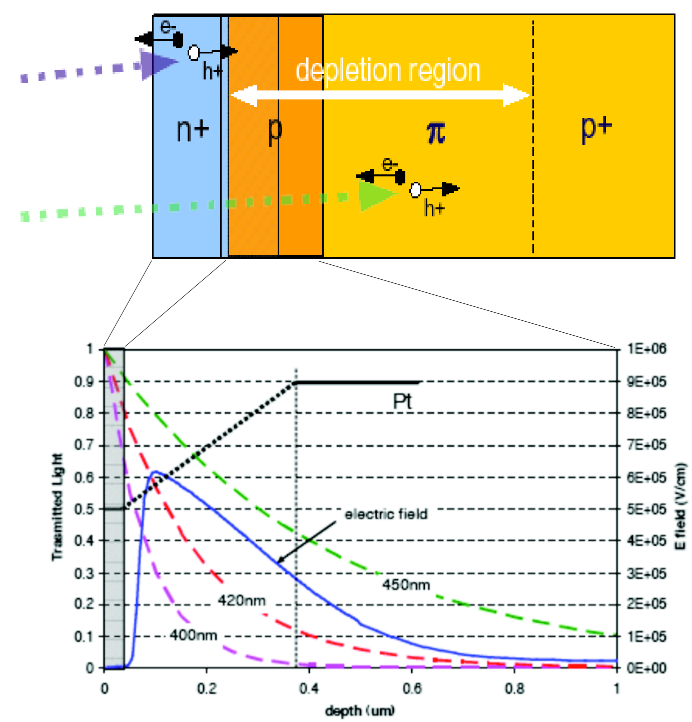

Quantitative comparison with models of time evolution of the avalanche and simulations: WORK in PROGRESS

Comparison with Photonique devices

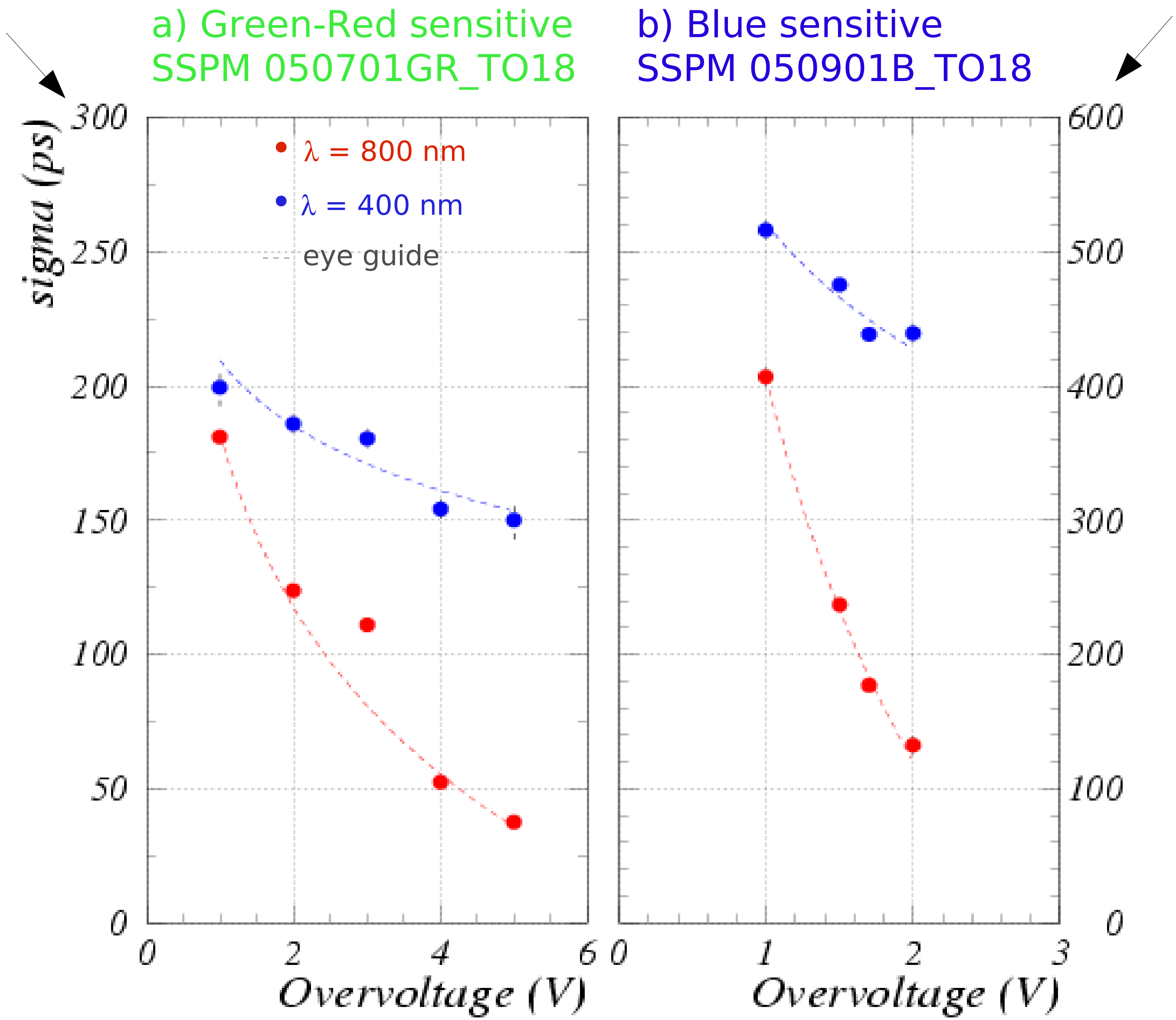

Better resolution for long wavelengths: ?

Two different structures:

a) n^+/p not particularly shallow junction

b) p^+/n even deeper junction

(?) WLS on entrance window

(?) kind of buried junction

Dependence on the light spot size

IRST devices:

Measurement with a pinhole in front of SiPM to have different laser light beam size.

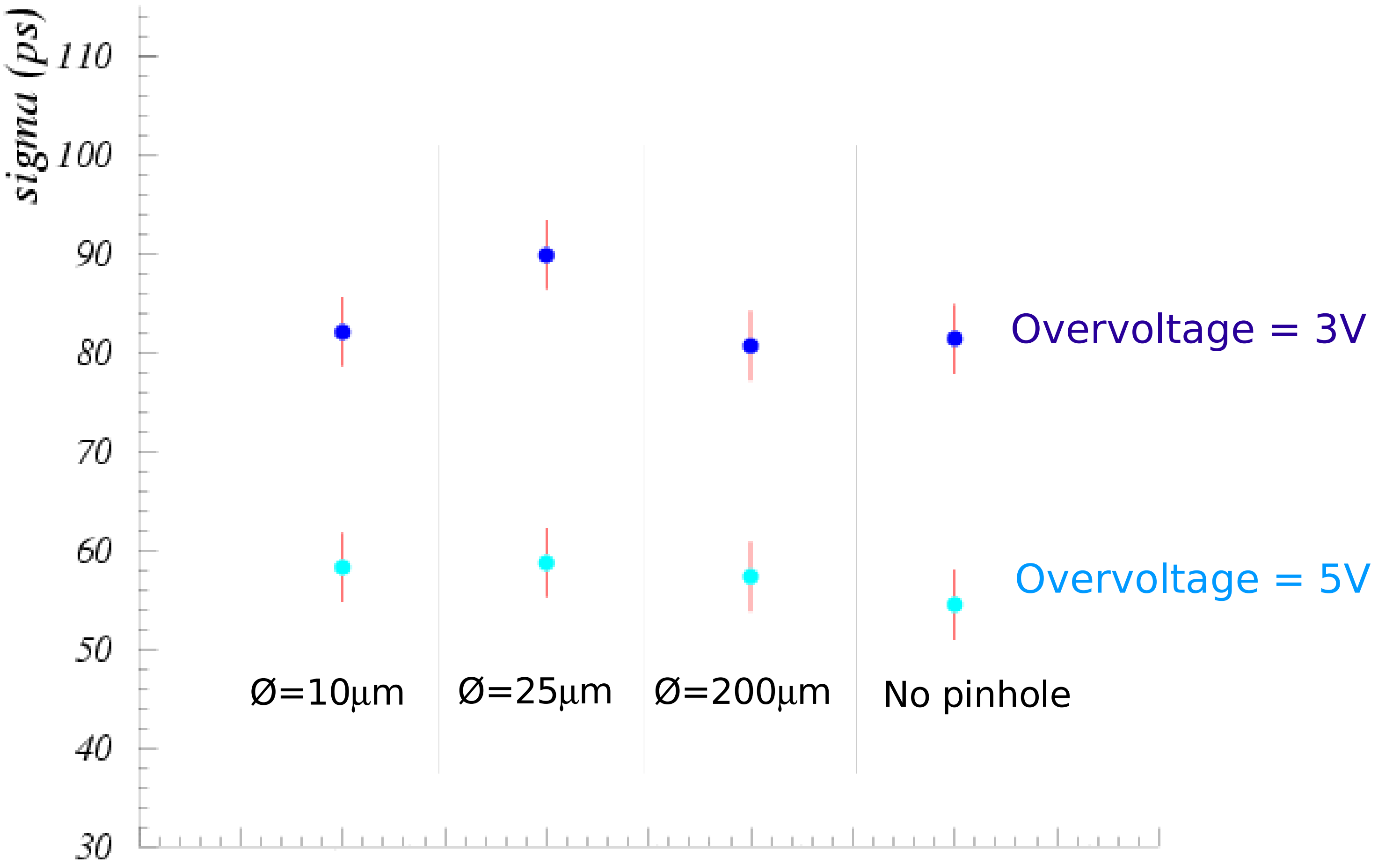

No relevant spread

→ Uniformity of rise-time among different cells

Dependence on the number of photons

IRST devices:

Poisson statistics:

$$\sigma_t \propto \sqrt{N_{pe}}$$

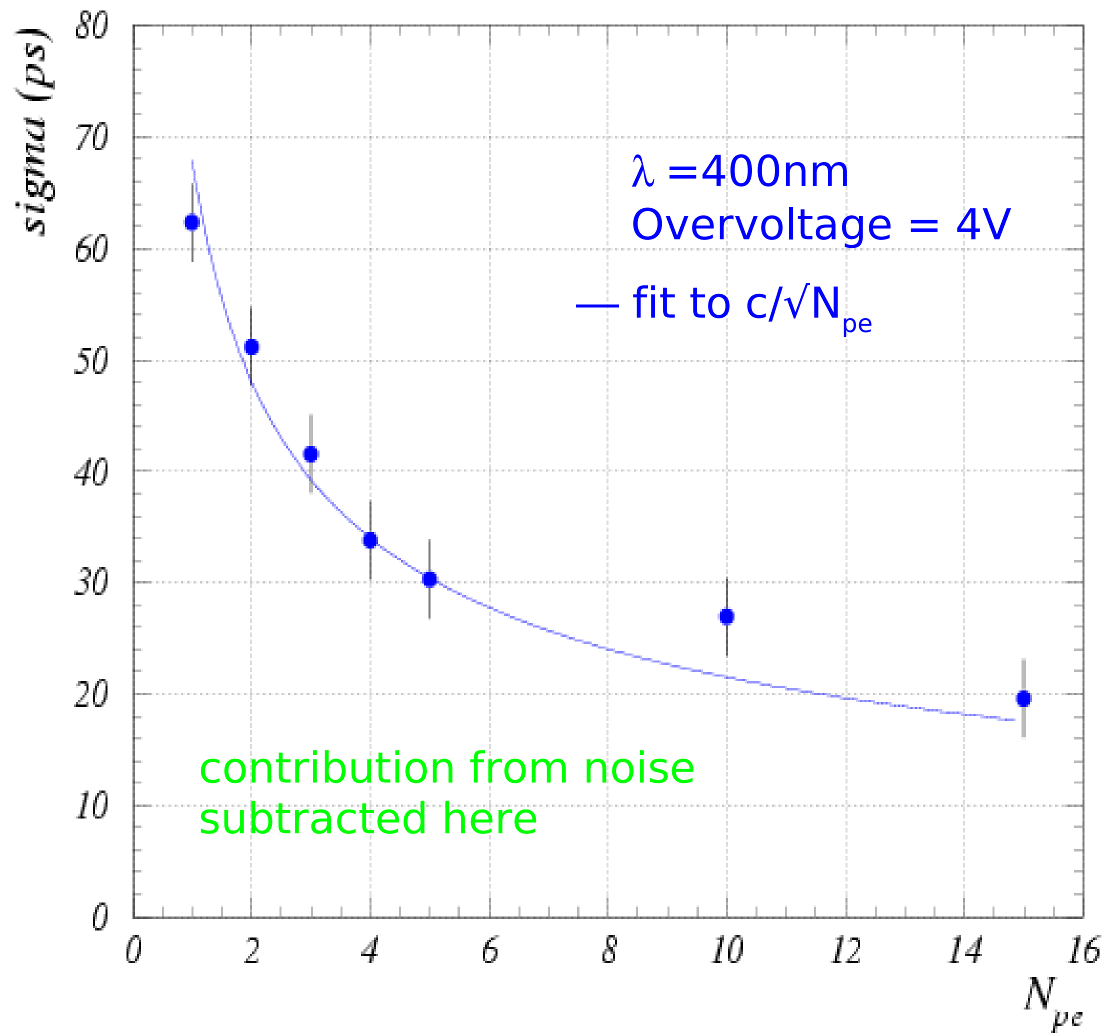

Simultaneous photons yielding 100pe might result in a resolution al the level of 10ps

(WORK is in PROGRESS to study timing with scintillators)

Energy resolution with LSO

^{22}Na spectrum with 1x1x10mm^3 LSO crystal (λ_{peak} ~ 420nm) coupled to a SiPM.

Energy resolution (at 0.511 MeV)

$\sigma_E/E \sim 9\%$

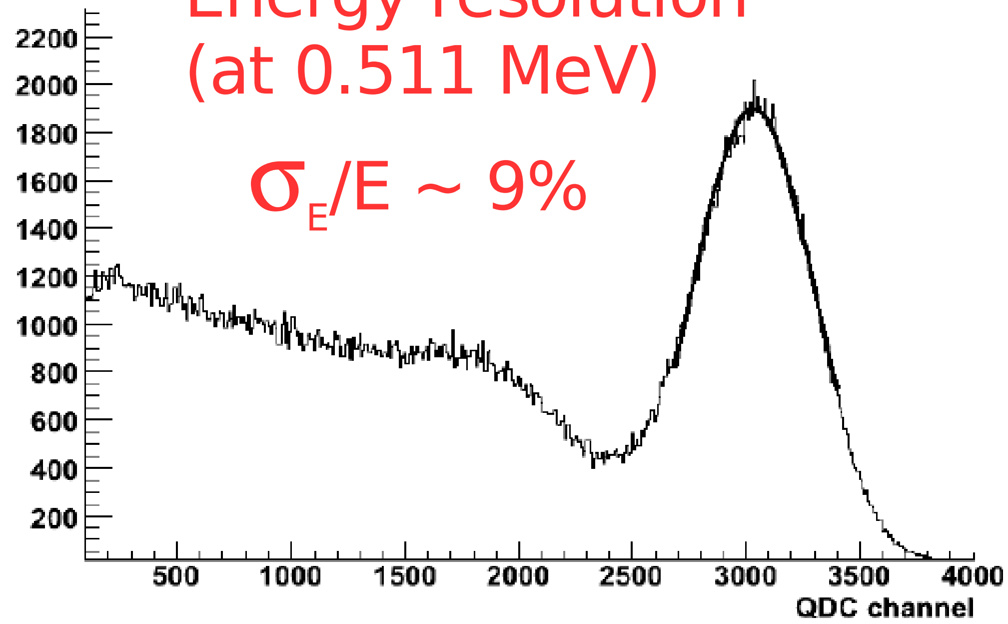

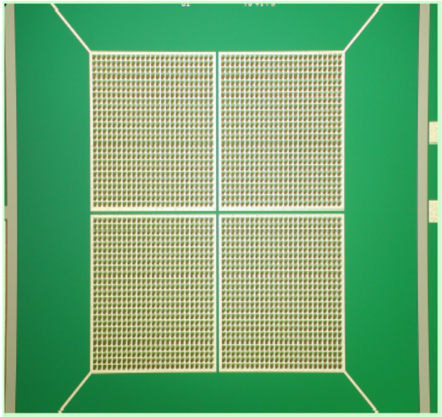

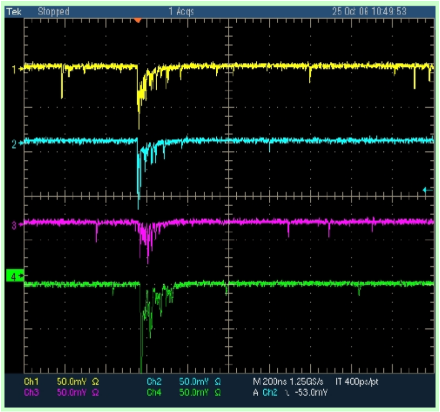

The first matrices of 2x2 SiPMs have been developed (IRST). Currently they are being tested (Pisa) by coupling to 2x2x20mm^3 LSO crystals.

G.LLosa et al. IEEE NSS 2006 CD record M06-88

Next steps and improvements

1) geometry optimization new layout ready with:

- increased fill factor ε_{geom} =
  40x40µm → 44%
  50x50µm → 50%
  100x100µm → 76%
- devices with larger area.

2) On the technological side:

- dark count reduction (gettering)
- buried-junction SiPM (photo-generation in the p-side of the junction → higher avalanche triggering probabilty due to electrons higher ioniz. rate)

  C.Piemonte, NIM A568 (2006) 224-232

Conclusions

SiPM might really replace PMT in many applications, due to their

- sensitivity to extremely low photon fluxes
- extremely fast response

IRST developed devices with excellent sensitivity to blue:

- devices working as expected
- very good reproducibility of the performances
- good yield
- good understanding of the device

Photo-detection efficiency (IRST devices):

- Quantum efficiency: > 95% in the blue region (optimized for 420nm)
- Triggering probability: growing linearly with overvoltage; could be optimized with buried-junction structure soon available
- Geometrical fill factor: 15-30% to be optimized $\rightarrow$ 44-76% soon available

Single photon timing resolution (IRST devices):

- σ_t at the level of 70ps for typical working overvoltage (4V)
- Non gaussian tails: no relevant slow tails for short wavelengths; long wavelengths show slow ($\tau <$ ns) tails (diffusion ?) contributing at 10-30%
- Work in progress on non gaussian tails, simulation, timing with scintillators

Additional information

Time differences distribution

Cross check: SiPM coupled to a fast plastic scintillator 2 x 2 x 15mm^3
Only the scintillator exposed to the laser blue light λ=400nm.
No direct laser light to the SiPM

$\rightarrow$ measurement of the scintillator decay tail

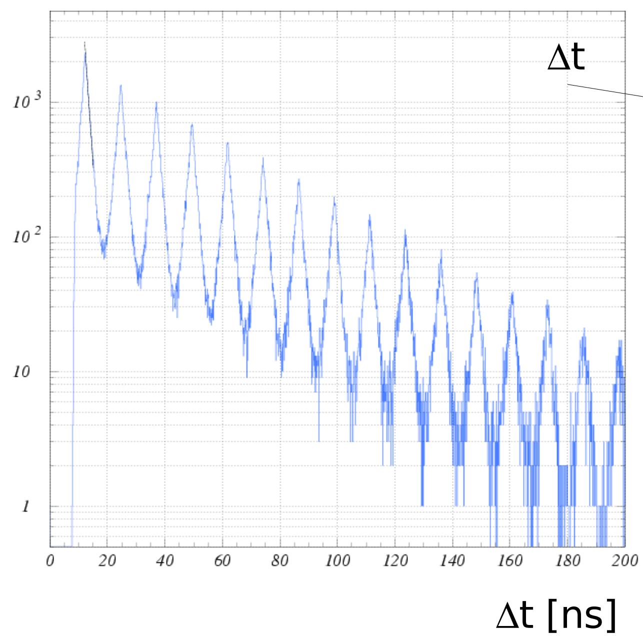

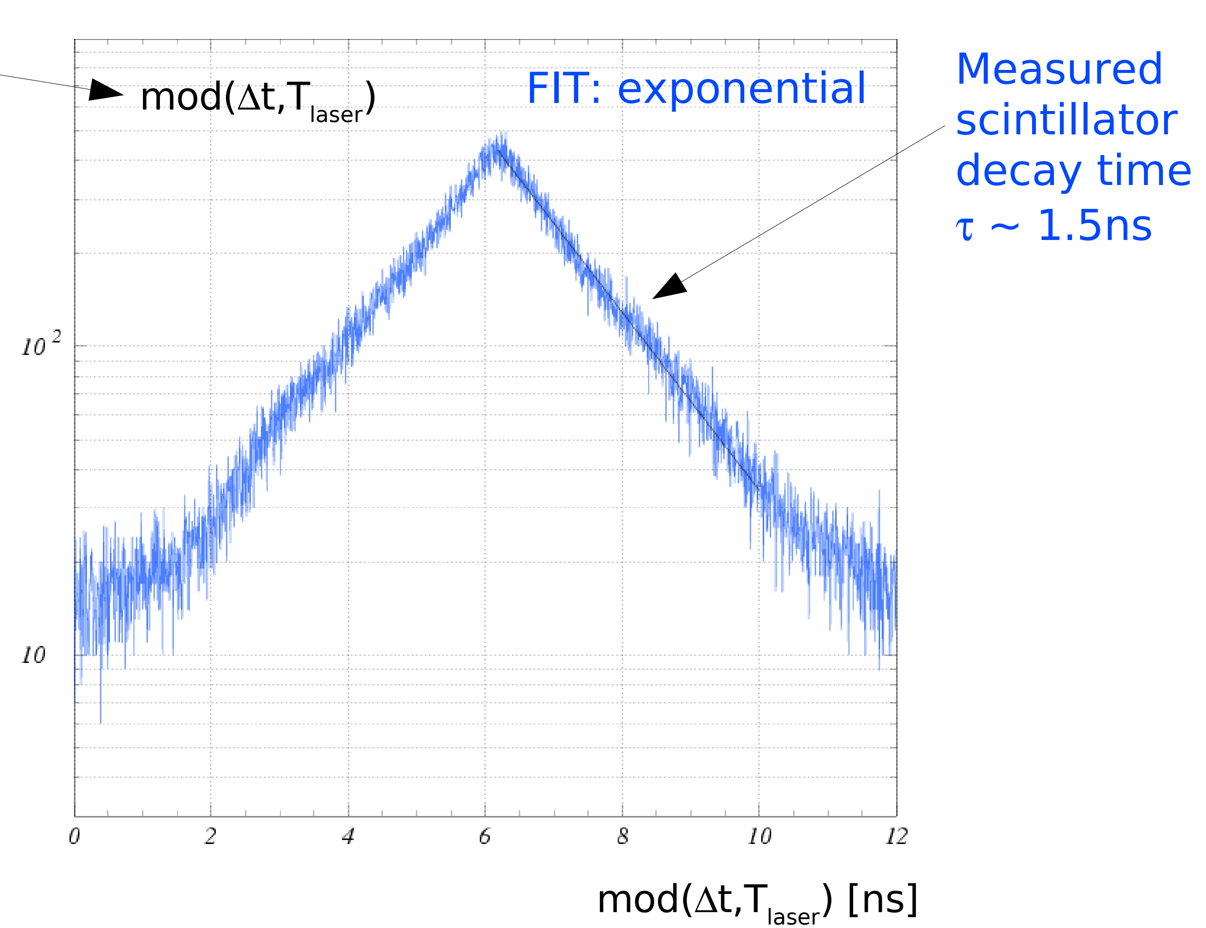

Operation principle of a SiPM

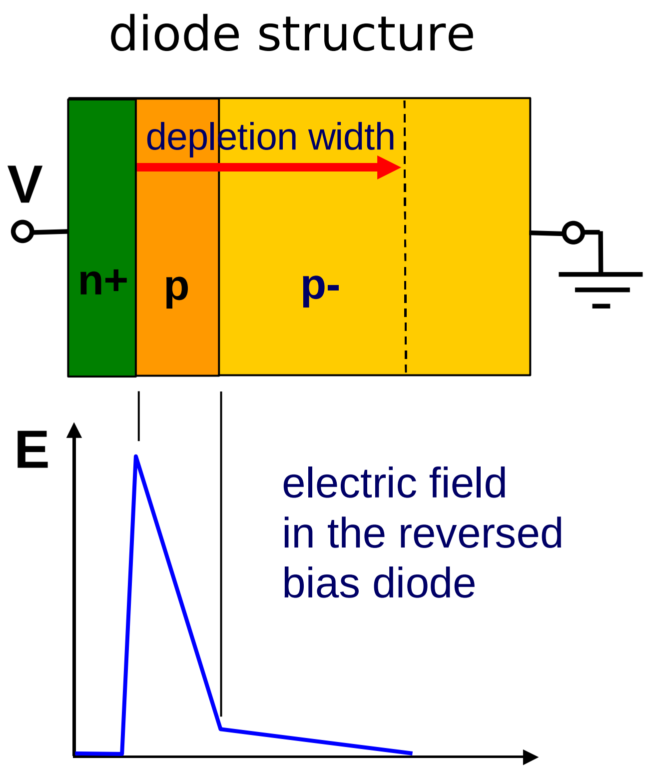

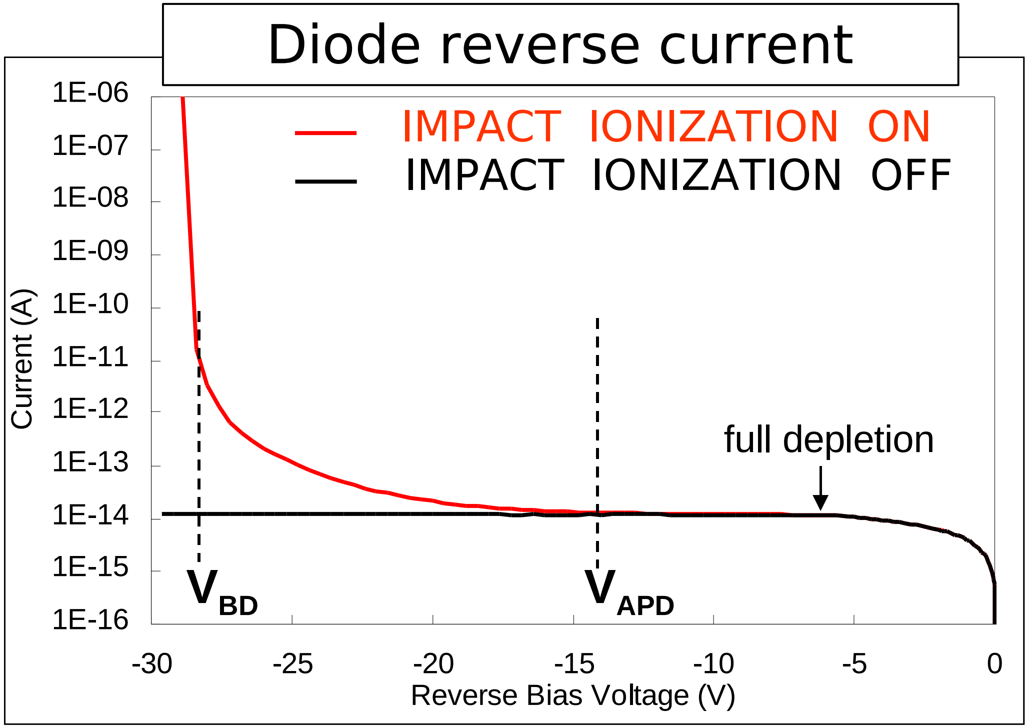

$V < V_{APD}$ => photodiode 1 collected pair/generated pair

$V_{APD} < V < V_{BD}$ => APD <M> collected pairs/generated pair

$V > V_{BD}$ => Geiger-mode APD inf. collected pairs/generated pair

Building block of a SiPM: Geiger-mode APD

The Geiger-Mode APD can be modeled with an electrical circuit and two probabilities:

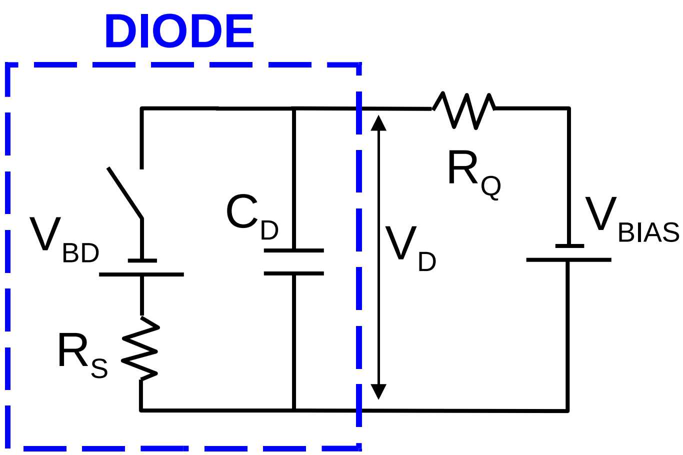

- C_d
- R_s
- V_{bd}

- R_q
- $V_{bias} > V_{bd}$

- P_{01}
- P_{10}

OFF condition:
switch open,
capacitance charged to V_{BIAS},
no current flowing

P_{01} = turn-on probability
probability that a carrier traversing the high-field region triggers the avalanche

ON condition:
avalanche triggered, switch closed
$\Rightarrow C_D$ discharges to V_{BD} with a time constant $R_S x C_D$, at the same time the external current grows to $(V_{BIAS}-V_{BD})/R_Q$

P_{10} = turn-off probability
probability that the number of carriers traversing the high-field region fluctuates to zero.

Gain in Geiger-mode APD

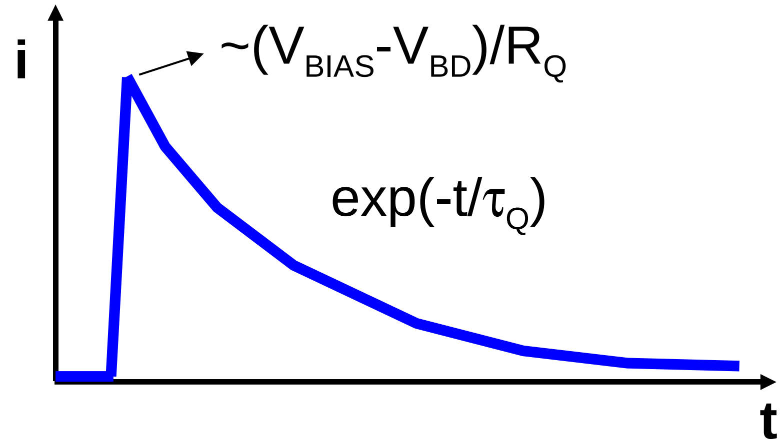

The first part of the signal is much faster than trailing edge, indeed:

1. $R_S * C_D << R_Q * C_D$
2. turn-off mean time is very short

Charge collected per event is the area of the exponential decay which is determined by circuital elements and bias.

It is possible to define a GAIN

$$\text{Gain} = \frac{I_{MAX} * \tau_Q}{q} = \frac{(V_{BIAS} - V_{BD}) * \tau_Q}{R_Q \, q} = \frac{(V_{BIAS} - V_{BD}) * C_D}{q}$$

This property is exploited in a Silicon photomultiplier

The SiPM structure

GM-APD gives no information on light intensity

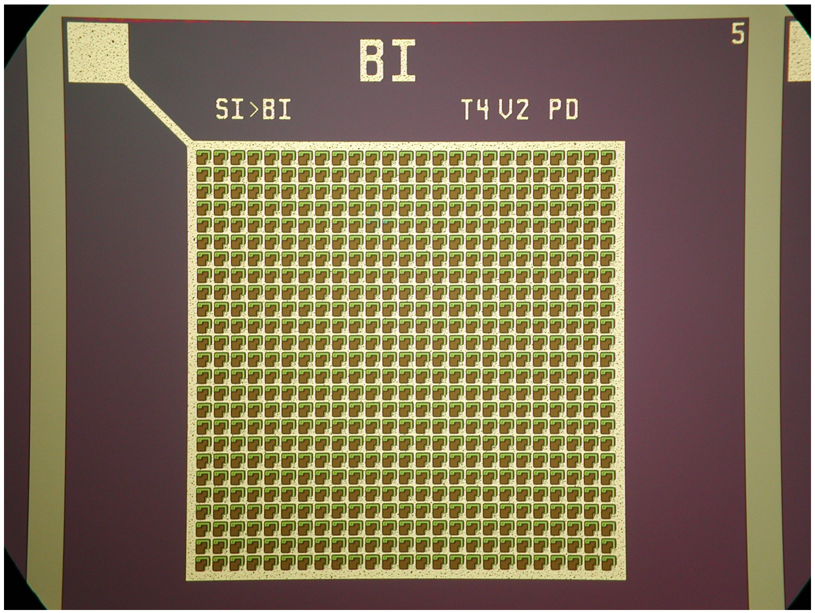

SiPM

first proposed by Golovin and Sadygov in the '90s

A single GM-APD is segmented in tiny micro GM-APD connected in parallel.

Each element is independent and gives the same signal when fired by a photon

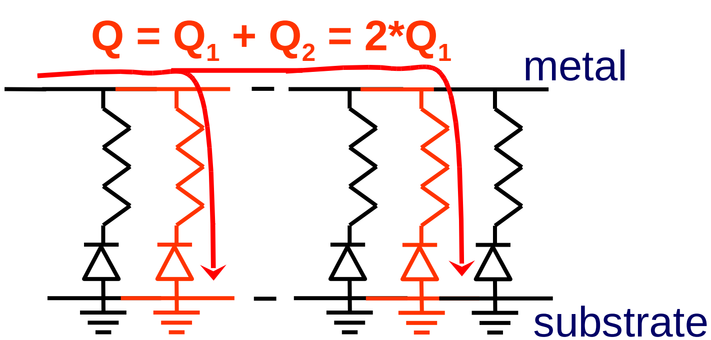

$\Rightarrow$ **output charge is proportional to the number of triggered cells that, for PDE=1, is the number of photons**

$V_{breakdown}$ vs T

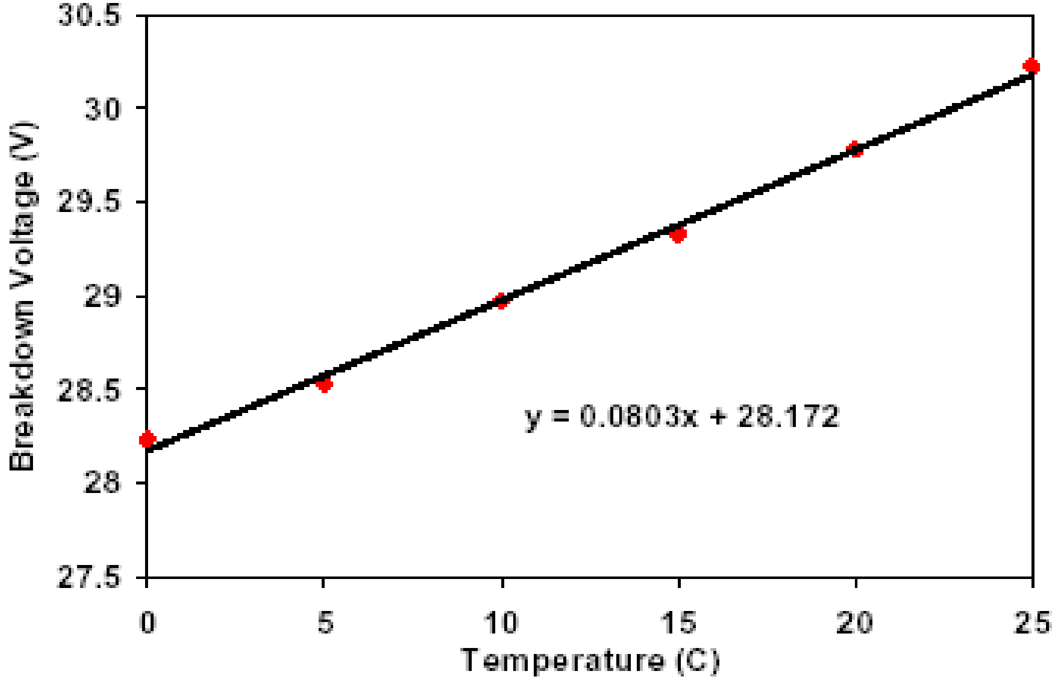

Discussion

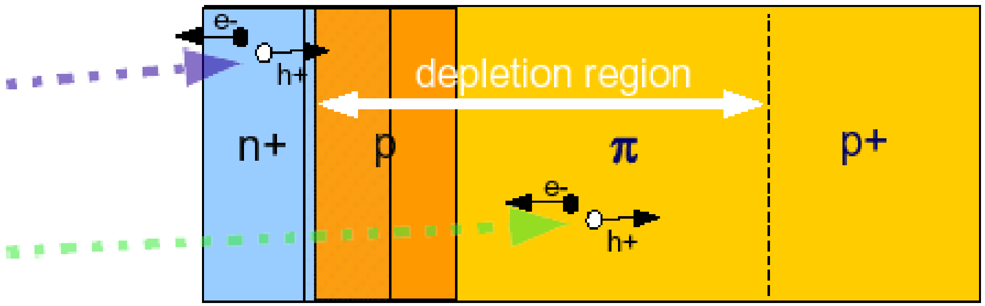

Pairs generated in the left side (short wl): e- collected, h+ trigger the avalange

Pairs generated in the right side (long wl): h+ collected, e- trigger the avalange

Rise time of the current generated by the device has two similar time scales:
* $\tau_{disch.} = R_S C_D$ discharge time constant (R of silicon and space charge)
* $\tau_{ava.}$ = Avalange building-up

Order of magnitude ~ few x 100ps

Fluctuations of rise time (jitter) due to:
1) Carrier generation position: ~ 10ps/um depletion region
2) Avalange multiplication (fluctuations) affecting the shape of the current leading edge: ~ 10 ps
3) Avalange lateral spreading (limited by space charge and quenching mechanism) affecting the shape of the leading edge: ~

Pairs generated in the left side (short wl) next to the high field region:
should give a "prompt" signal: only (2)+(3) involved

Pairs generated in the right side (long wl):
also mechanism (1) involved
which should account for the observed difference in blu/red response